

Bending strain-driven modification of surface reconstructions: Au(111)

U. Tartaglino^{1,2,*}, E. Tosatti^{1,2,3}, D. Passerone^{4,1,2}, and F. Ercolessi^{5,1,2}

¹ *SISSA, Via Beirut 2, I-34014 Trieste, Italy*

² *Unità INFN/SISSA*

³ *ICTP, Strada Costiera 11, I-34100 Trieste, Italy*

⁴ *CSCS, Galleria 2, CH-6928, Manno, Switzerland*

⁵ *Dip. di Fisica, Università di Udine, Via delle Scienze 208, I-33100 Udine, Italy * FAX: +39-040-3787528; e-mail: tartagli@sissa.it*

(October 26, 2018)

Strain can affect the morphology of a crystal surface, and cause modifications of its reconstruction even when weak, as in the case of mechanical bending. We carried out calculations of strain-dependent surface free energy and direct bending simulations demonstrating the change of incommensurate reconstruction in Au(111) under strain, in good agreement with recent data. Time-dependent strain should cause a sliding of the topmost layer over the second, suggesting an interesting case of nanofriction. Bending strain could also be used to fine tune the spacing of selectively absorbed nanoclusters.

PACS numbers: 68.35.Bs, 68.35.Gy, 68.35.Md

Crystal surfaces often break their ideal bulk-like symmetry, even in the absence of adsorbates, to lower their free energy through the so-called reconstructions. Temperature, adsorbate coverage and (in electrolytes) electrochemical potential [1] cause these reconstructions to evolve, either continuously or through two-dimensional phase transitions [2]. Work on semiconductor surfaces [3–5] indicated that external strain too can drive changes in surface reconstruction. In this letter we present theory and simulations indicating that reconstruction changes at an incommensurate metal surface like Au(111) can be provoked by application of strain, even with the weak strains attainable by bending a platelet or slab. When compared with very recent data, which appeared while this paper was being reviewed, the quantitative agreement is remarkable. We propose a possible application of this fine effect to selective adsorption of nanostructures on this surface. Because the strain-induced reconstruction changes involve a continuous change of first-layer lateral atom density, time-dependent bending strain will also drive a kind of incommensurate nanofriction.

We introduce in a semi-infinite crystal a uniform strain $\lambda\varepsilon_{\alpha\beta}$, λ increasing from 0 to 1. The surface free energy change, equalling the surface work, is obtained through thermodynamic integration:

$$\Delta(\gamma A) = W_s = \int_A dA \int_0^1 \tau_{\alpha\beta}^{\text{surf}}(\lambda) \varepsilon_{\alpha\beta} d\lambda$$

where γ is the surface free energy per unit area, A the area, $\tau_{\alpha\beta}^{\text{surf}}$ the (strain dependent) surface stress, and α, β span the (x, y) in-plane coordinates. If the surface free energies (per unit area) of two different reconstructions 1 and 2 satisfy $\gamma_1^0 < \gamma_2^0$, then in the absence of strain state 1 prevails over 2. However, their respective surface stress tensors generally differ, and free energies will thus vary with different slopes under strain, possibly leading

to $\gamma_1 > \gamma_2$. We are interested in a detectable modification of reconstruction periodicity, particularly if obtainable even with the weak strains provided by mechanical bending.

To explore that, we choose the promising example of Au(111) as our test case. Au(111) displays a well documented $(L \times \sqrt{3})$ reconstruction [6], ($L \approx 22.5$ in ordinary conditions). It is promising because its long incommensurate period L should readily be changeable by a small but detectable amount. The $(L \times \sqrt{3})$ pattern, commensurate along $\langle 1\ 1\ \bar{2} \rangle$, is incommensurate in the orthogonal $\langle 1\ \bar{1}\ 0 \rangle$ direction, where the reconstruction consists of a succession of hcp and fcc stripes, separated by sharp soliton-like boundaries, due to an extra row of atoms for each period L of reconstruction. X-Ray diffraction experiments [7] show as temperature is raised from 300 to 800 K, a *continuous* shift of the periodicity L from about 22.5 to 20.9, which confirms the incommensurability. It also indicates a denser and denser surface at higher temperatures, a kind of negative expansion coefficient (probably arising, as in the case of Au(100) [8,9], to compensate for a large outwards thermal relaxation of the first layer). Here we shall describe how an external strain too can change the periodicity L of Au(111).

To describe the initial $(L \times \sqrt{3})$ reconstruction we use an empirical many-body classical potential, the glue model [10], known to describe reasonably well all the gold surfaces. In the glue model, the ground state of Au(111) is properly reconstructed, though with a somewhat shorter $T = 0$ periodicity $L = 11$ [11]. The difference between that and the experimental $L = 22.5$ is a purely numerical discrepancy that can be corrected for, and of no fundamental significance. The long range “heringbone” secondary superstructure also well known on this surface [7] is much more delicate involving far smaller energies, and will not concern us any further here. All calculations and simulations are conducted for thin crys-

tal slabs where strain is introduced by simulated bending [12], as in real-life experiments [1] (although of course our theoretical slabs are far thinner).

Calculations of the surface free energy change under strain start with an N -layer fcc (111) slab, its two faces ($L \times \sqrt{3}$) reconstructed with different periodicities L and L' . That is obtained by addition of one extra $[1\ 1\ \bar{2}]$ row of surface atoms every L , followed by relaxation [11]. We carry out molecular dynamics simulations of about 1 ns at 100 K, to obtain by standard methods [13] the average stress tensor $\sigma_{\alpha\beta}$. From the same simulation we also extract a *layer-resolved* stress profile $\tau_{\alpha\beta}(z_l)$, defined as the force per unit length acting in layer l :

$$\tau_{\alpha\beta}(z_l) = -\frac{1}{A} \left\langle \sum_{i \in l} \left(\frac{p_{\alpha i} p_{\beta i}}{m_i} + \frac{1}{2} \sum_j \frac{\partial U}{\partial r_{ij}} \frac{r_{ij, \alpha} r_{ij, \beta}}{r_{ij}} \right) \right\rangle,$$

where i runs over the atoms of layer l , j spans all the atoms, and U is the potential energy, a function of the interatomic distances (this formula is easily modified for application to a bent slab [14]). The elastic bending work is done in our case by τ_{yy} , $y \equiv [1\ \bar{1}\ 0]$ being the strained direction, orthogonal to the solitons.

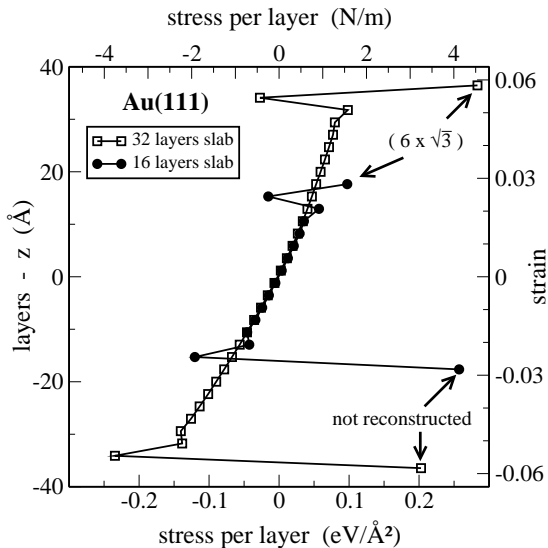


FIG. 1. Layer-resolved stress profiles of two Au(111) slabs with 16 and 32 layers, subjected to the same bending curvature. Note the large surface stress and the sub-surface oscillations. The non linear bulk stress profile is due to anharmonicity.

The bent slab stress profile obtained for $L = 6$, $L' = \infty$ (at $T = 100$ K) is shown in Fig. 1. The smoothly varying bulk-like stress in the interior of the slab develops at the surface a sharp oscillation, swinging from compressive in the second layer to tensile in the first layer. As shown by comparison of two different slabs with the same curvature but different thicknesses, $N = 16$, and 32, the surface stress of the thinner slab can be immediately computed by subtracting off the corresponding bulk-like

stress of the thicker slab. The bulk stress $\tau_{yy}^{(\text{bulk})}(z)$ deviates from the linearity for increasing strain in a way that is very well described by a parabolic fit, the nonlinearity due to anharmonicity. The layer-resolved surface stress is then obtained as $\tau_{yy}^s(z_l) = \tau_{yy}(z_l) - \tau_{yy}^{(\text{bulk})}(z_l)$. Repeating calculations for increasing curvature k we obtain the curvature-dependent surface stress. This approach, we note, will give free energy differences, fully inclusive of the entropic term. Finally the free energy change as a function of strain is obtained by integrating [14]:

$$W_s = \sum_{l \in \text{layers}} \int_0^k d\kappa \tau_{yy}^s(z_l) \frac{d\varepsilon_{yy}(z_l)}{d\kappa}$$

Likewise, the total surface stress can be obtained as $\tau_{\alpha\beta}^{\text{surf}}(k) = \sum_{l \in \text{layers}} \tau_{\alpha\beta}^s(k, z_l)$.

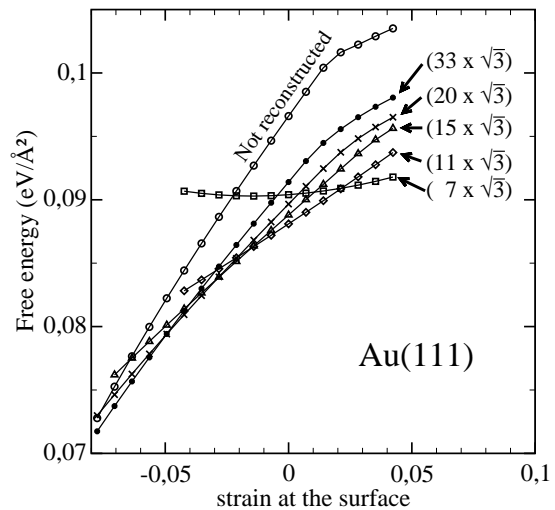


FIG. 2. Free energies at 100 K of various $(L \times \sqrt{3})$ Au(111) surface reconstructions calculated as the strain is changed through bending. (The free energy values at zero strain are arbitrarily set at their independently obtained $T = 0$ values). The predicted strain induced drift of L can be extracted from the lowest envelope of these curves.

Fig. 2 displays our main result: the strain-induced free energy variation of several different $(L \times \sqrt{3})$ reconstructions of Au(111) at $T = 100$ K. The strain dependence found for free energy is relatively large, of order $2 \text{ meV}/\text{\AA}$ (about 1% of the total surface free energy) for 1% strain. By comparison with the absolute zero-temperature surface energy differences at zero strain, independently calculated (and used in Fig. 2 to fix the unknown relative position of curves, thus neglecting an entropy term, hopefully small at low temperatures) we find that $0.18 \text{ meV}/\text{\AA}$ is roughly the surface free energy difference between periodicities L and $L + 1$ for L around 20 in Au(111). By interpolating Fig. 2 we find that a change of periodicity from, say, $L = 23$ to $L = 24$ can in principle be provoked by a compressive surface strain of order 0.2%. More generally, strain will cause a periodicity drift determined by the lower envelope of all the curves: posi-

tive (tensile) strain decreasing L , negative (compressive) strain increasing it. Eventually for a theoretically very large strain $L = \infty$ would be reached, where the reconstruction itself disappears. That strain, of order -2% in Au(111) (see below), might however be too large to be achieved by bending.

Our predictions, based on free energies, find a first confirmation in a computer experiment, consisting of a realistic molecular dynamics simulation, based on introducing a bending strain in the same slab geometry previously used for the surface stress calculation. If we start out with two identically reconstructed surfaces, bending strain should cause L to spontaneously increase on the concave face, and decrease on the convex one. The simulation must however overcome a technical problem, connected with particle conservation. A change of reconstruction periodicity L implies a change of first-layer lateral surface density, equal to $(1 + 1/L)$ times the density of an unreconstructed layer. The initially flat, defect free reconstructed surface should, under bending, spontaneously expel atoms from the top layer to form islands on the concave face, while opening craters that expose a portion of the layer below on the convex face [15]. Such phenomena are slow, needing times much longer than the typical simulation nanosecond. Because of that, it would seem that molecular dynamics simulation should be abandoned. A practical way out of this problem [16] is to include a loose grid of steps in the starting configuration, which amounts to simulate a very close vicinal face rather than the original (111) surface.

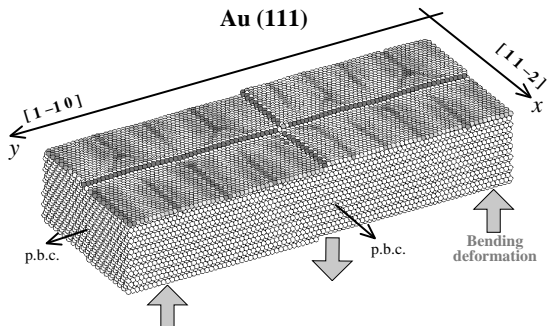


FIG. 3. The upper half of the simulation slab, with two orthogonal steps. Periodic boundary conditions require no extra steps at the boundaries. The grayscale reflects atomic coordination: atoms at the solitons between fcc and bcc regions appear darker.

Our realization, shown in Fig. 3, comprises four sub-terraces of heights 0, 1, 1, 2, separated by steps, and connected one with another across suitably shifted boundary conditions [16]. No other steps occur at the boundaries, hence the four sub-terraces constitute in reality a single large terrace. The terrace size used is $88d \times 20\sqrt{3}d$, with d the nearest neighbour distance. With this geometry we can carry out various simulations, bending an initially flat surface and unbending an initially bent surface. In order to speed up kinetics, the temperature is raised well

above room temperature, up to about $T = 600K$.

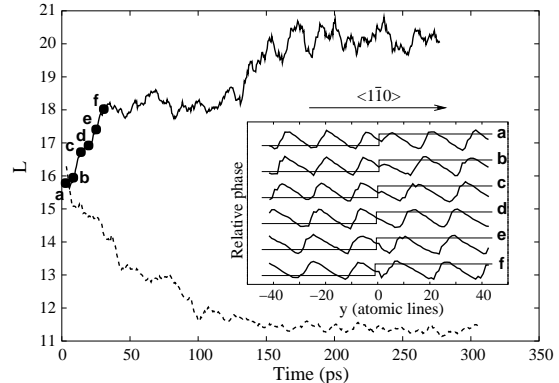


FIG. 4. Time evolution of the reconstruction periodicity, from a nonequilibrium starting point with $L = 16$, towards equilibrium. Solid line: bent slab with a compressive surface strain of -4.7% . Dashed line: flat slab with zero surface strain. Geometry as in Fig. 3, $T = 800 K$. Inset: detail of the phase difference between the atoms of the first two layers, at selected instants of time during the bending. Note that the step, indicated schematically at each of the instants, has moved slightly to the left in correspondence with the increase of L (decrease of lateral density). The excess soliton is absorbed at the step upper rim between instants (a) and (c).

Representative simulation results are illustrated in Fig. 4, where the continuous drift of reconstruction periodicity for a surface initially reconstructed with L around 16 is demonstrated for two different situations, a large compressive surface strain, and zero strain respectively, the former obtained through simulated bending. The periodicity drift from 16 to about 20 and from 16 to about 11 in the two cases is in good agreement with the free energy prediction of Fig. 2. The inset details the behavior of the phase of the topmost atom layer lattice relative to the bulk-like second layer (modulo 2π) as seen on the bent slab at selected instants of time. Data are averaged along the $[11\bar{2}]$ direction to reduce the noise due to thermal excitation: averaging explains why the phase jumps around 2π are replaced by a smooth behaviour. We find that the periodicity changes are actuated through the appearance (or disappearance) of solitons, nucleated preferentially at the upper rim of the surface step, where atoms possess the lowest coordination.

Experimentally, attempts to provoke and observe by STM surface reconstruction modifications by bending, have been carried out recently, precisely on Au(111). Because the strains attained are small they were found to affect mostly the secondary structure. An early unpublished report by Huang et al. [17], described strain-induced removal of the wrongly oriented domains of the secondary herringbone structure with strains as small as 1.3×10^{-5} , with occasional removal of the whole reconstruction. Newer data of Schaff et al. [18] show that the secondary structure is again removed but the $(L \times \sqrt{3})$ reconstruction survives at least up to a maximum com-

pressive strain of 0.4%. By closer examination of their data we note that under strain, exerted at an angle of 30° with respect to the solitons, there is evidence of a drift of periodicity L from about 23 to about 25. We can directly compare that with our calculations. We find that the calculated L -dependent surface free energy for variable bending is well fitted by a Pokrovskii-Talapov form [2] $\Delta E = -a/L + b/L^3$, where a is the cost of solitons and b reflects their mutual interaction $\propto 1/L^2$. Here $a(\varepsilon) = a' \cdot (\varepsilon - \varepsilon_c)$ will vanish at a critical strain ε_c , so that $L = K(\varepsilon - \varepsilon_c)^{-1/2}$, where $K = \sqrt{3b/a'}$. Based on our computed surface energies and anisotropic surface stress tensor, we derived K and ε_c for arbitrary strain direction, so as to compare the experimental drift with calculated periodicity changes (Fig. 5). The agreement obtained is very encouraging, fully supporting our qualitative expectations, and demonstrating the applicability of the proposed mechanism of surface modification under bending strain.

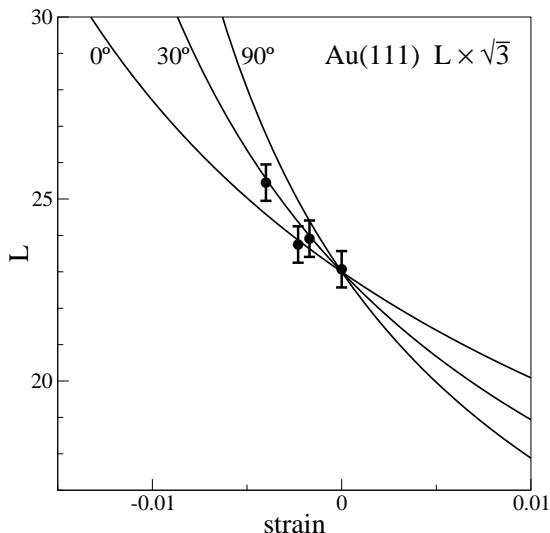


FIG. 5. Change of Au(111) reconstruction period L as a function of applied strain. Solid lines, are theoretical predictions, in the form $L = K(\varepsilon - \varepsilon_d)^{-1/2}$, for strains orthogonal ($\theta = 90^\circ$, $K = 2.84$, $\varepsilon_d = -0.0153$), oblique ($\theta = 30^\circ$, $K = 3.34$, $\varepsilon_d = -0.0210$) and parallel ($\theta = 0^\circ$, $K = 4.12$, $\varepsilon_d = -0.0323$) to the $[11\bar{2}]$ oriented solitons. These parameters best fit our simulation results, with a shift in strain, to make the $L = 23$ point correspond to strain $\varepsilon = 0$. Data points were extracted from the STM images of ref. [18], where the strain direction was $\theta = 30^\circ$.

The strain-induced reconstruction changes described above can lead to potentially interesting consequences and applications. In a surface that is perturbed by a time-dependent strain, there will be as a consequence a sliding nanofriction of the incommensurate reconstructed top layer of Au(111) against the regular second layer. For example, an oscillatory bending would result according to Fig. 4 in a corresponding variation of L , driving an oscillatory sliding of the first layer onto the second. A pinned state of the top layer will imply a threshold

strain magnitude to actuate the sliding. When the sliding occurs, a surface nanofrictional contribution should appear as a part of the mechanical damping of a Au(111) platelet. Among the applications, there could be the possibility to tune through bending strain the spacing between deposited nanoclusters. Recently, deposition of 1-nitronaphthalene (NN) nanoclusters on a stepped Au(111) surface has revealed [19] that at the low coverage adsorption at the step is favored in the fcc zones of the $L \times \sqrt{3}$ reconstruction pattern and unfavored in the hcp zones, and in this way, stripes can be produced. The distance among the stripes could in principle be changed upon bending, with interesting consequences in the field of miniature device fabrication.

This work was supported through contracts INFM PRA NANORUB, and MIUR COFIN. We thank P. Zeppenfeld and O. Schaff for bringing their work to our attention, and for illuminating discussions.

-
- [1] H.Ibach, Surf. Sci. Reports **29**, 193 (1997)
 - [2] B.N.J.Persson, Surf. Sci. Reports **15**, 1 (1992)
 - [3] D.Vanderbilt, Phys. Rev. Lett. **59**, 1456 (1987)
 - [4] D.Vanderbilt, Phys. Rev. **B R36**, 6209 (1987)
 - [5] F.Liu and M.G.Lagally, Phys. Rev. Lett. **76**, 3156 (1996)
 - [6] Y.Tanishiro, H.Kanamori, K.Takayanagi, K.Yagi, and G.Honio, Surf. Sci. **111**, 395 (1981); U.Harten, A.M.Lahee, J.P.Toennies, and Ch.Wöll, Phys. Rev. Lett. **54**, 2619 (1985), and references therein.
 - [7] A.R.Sandy, S.G.J.Mochrie, D.M.Zehner, K.G.Huang and D.Gibbs, Phys. Rev. B **43**, 4667 (1991)
 - [8] K.Yamazaki, K.Takayanagi, Y.Tanishiro, and K.Yagi, Surf. Sci. **199**, 595 (1988)
 - [9] D.Gibbs, B.M.Ocko, D.M.Zehner and S.G.J.Mochrie, Phys. Rev. B **42**, 7330 (1990)
 - [10] F.Ercolessi, M.Parrinello, and E.Tosatti, Phil. Mag. **A58**, 213 (1988)
 - [11] F.Ercolessi, A.Bartolini, M.Garofalo, M.Parrinello, and E.Tosatti, Surf. Sci. **189/190**, 636 (1987).
 - [12] D.Passerone, E.Tosatti, G.L.Chiarotti, and F.Ercolessi, Phys. Rev. B **59**, 7687 (1999)
 - [13] M. W. Ribarsky and U. Landman, Phys. Rev. B **38**, 9522 (1988)
 - [14] U. Tartaglino, D. Passerone, E. Tosatti and F. Di Tolla, Surface Science, **482-485**, 1331 (2001)
 - [15] D.Passerone, F.Ercolessi, and E.Tosatti, Surf. Sci. **377-379**, 27 (1997)
 - [16] D.Passerone, F.Ercolessi, U.Tartaglino and E.Tosatti, Surf. Sci. **482-485**, 418 (2001)
 - [17] L.Huang, P.Zeppenfeld, and G.Comsa, private communication
 - [18] O.Schaff, A.K.Schmid, N.Bartelt, J.de la Figuera and R.Q.Hwang, Mat. Sci. Eng. **A 319-321**, 914 (2001)
 - [19] M.Vladimirova, M.Stengel, A.De Vita, A.Baldereschi, M.Böhringer, K.Morgenstern, R.Berndt, and W.-

